Probabilistic Thresholds for Landslides Warning by Integrating Soil Moisture Conditions with Rainfall Thresholds

Binru Zhao[1,2], Qiang Dai[3,2], Dawei Han[2], Huichao Dai[1], Jingqiao Mao[1], Lu Zhuo[2]

[1]College of Water Conservancy and Hydropower Engineering, Hohai University, Nanjing, China.

[2]Department of Civil Engineering, University of Bristol, Bristol, UK.

[3]Key Laboratory of VGE of Ministry of Education, Nanjing Normal University, Nanjing, China.

Corresponding author: Qiang Dai (bz17336@bristol.ac.uk)

Keywords

probabilistic thresholds, landslides warning, soil moisture, rainfall thresholds

Abstract

Various methods have been proposed to define the rainfall thresholds for the landslide prediction. Once the appropriate threshold is determined, it remains the same regardless of the antecedent soil moisture conditions. However, given the important role of the antecedent soil moisture in the initiation of landslides, it is considered if the rainfall threshold level varies according to the antecedent soil moisture conditions, the prediction performance will be improved. Therefore, in this study we propose a probabilistic threshold to integrate antecedent soil moisture conditions with rainfall thresholds. In order to take into account the conditions with landslides and without landslides, the Bayesian analysis is applied to estimate the landslide occurrence probability given the various combinations of two factors: the antecedent soil moisture and the severity of the recent rainfall event. These combinations are then divided into conditions that are likely to trigger landslides and those unlikely to trigger landslides by comparing their probabilities with a critical value. In this way, the probabilistic threshold is determined. Here the soil moisture is estimated using the distributed hydrological model, and the severity of the rainfall event is characterized by the cumulated event rainfall-rainfall duration (ED) thresholds with different exceedance probabilities. The proposed approach was applied to a sub-region of the Emilia-Romagna region in northern Italy. The results show that the probabilistic threshold has a better prediction performance than the ED rainfall threshold, especially in terms of reducing false alarms. This study provides an effective approach to improve the prediction capability of the ED rainfall threshold, benefiting its application in the landslide prediction.

1 Introduction

Landslides are one of the most common natural hazards in mountain regions, with a high frequency of occurrence and serious threat to life and property. Being able to predict landslide occurrences in time and space is of great importance for the hazard management, which can help mitigate the influence caused by landslides. The initiation of landslides is the result of multiple factors, including intrinsic

factors that determine soil structure and slope stability (like topography, geology and soil regolith) and extrinsic factors that can change soil shear strength and lead to slope failures ultimately (like rainfall, earthquakes, and volcanoes). Landslide susceptibility maps are widely used to assess the relative likelihood of future landslides of an area based on the intrinsic factors that are responsible for the slope instability. As for the extrinsic factor, rainfall is the most common triggering factor for landslides, and the rainfall threshold is the most popular tool used to study the relationship between rainfall and landslide occurrences.

Rainfall thresholds are defined as the minimum rainfall conditions that are likely to trigger landslides (Guzzetti et al., 2008). For what concerns the rainfall variables, the most common combinations are "intensity-duration (ID)", "cumulated event rainfall-rainfall duration (ED)" and "antecedent rainfall". The ID threshold was firstly proposed by Caine (1980) to construct a global threshold for the occurrence of shallow landslides. Since then, the ID threshold is widely used at the local, regional and global scales (Guzzetti et al., 2007; 2008; Segoni et al., 2018). The ED threshold is more widely used in recent studies, especially those carried out in the landslide-prone areas of Italy (Gariano et al., 2015; Peruccacci et al., 2012; 2017). As for the threshold relying on the antecedent rainfall conditions, the antecedent period varies a lot in the published literature. Chleborad et al. (2008) and Scheevel et al. (2017) combined the recent 3-day rainfall and antecedent 15-day rainfall. Lee et al. (2015) considered the daily and 3-day cumulated rainfall. In addition to the direct use of rainfall information, some authors also employed the antecedent rainfall indexes as a proxy of the antecedent wetness condition, like the Antecedent Precipitation Index (Glade et al., 2000). The approach of defining rainfall thresholds ranges from visual fits (Caine, 1980) to some statistical methods, like the method based on Bayesian inference (Guzzetti et al., 2007; 2008) and the frequentist approach (Brunetti et al., 2010). For these methods, rainfall thresholds are defined deterministically with rainfall events that have triggered landslides. Probabilistic rainfall thresholds are also explored by Berti et al. (2012) using a

Bayesian approach, where both rainfall events with landslides and those without landslides are taken into consideration.

The rainfall thresholds can be identified as two categories according to their objectives (Lagomarsino et al., 2015; Segoni et al., 2018). One is to identify the minimum rainfall conditions that are likely to trigger landslides (minimum thresholds hereafter), and the other aims at achieving the balance between correct predictions and incorrect predictions when forecasting landslide occurrence in early warning systems (warning thresholds hereafter). Although the minimum thresholds are mostly determined in the previous studies, they are very conservative, which could cause a high number of false alarms. To apply rainfall thresholds to the landslide early warning systems, more and more studies try to define the warning thresholds that could provide good prediction performance. For this purpose, thresholds with different exceedance probabilities are evaluated with the help of contingency tables, skill scores, and the receiver operating characteristic (ROC) approach (Giannecchini et al., 2012; Gariano et al., 2015; Lagomarsino et al., 2015). Although the warning thresholds can be defined in this way, once the threshold is determined, it remains the same regardless of the antecedent soil moisture conditions. However, it is considered if the warning threshold varies according to the antecedent soil moisture conditions, the prediction performance will be improved. The landslide occurs due to the accumulation water in the subsurface which could alter the pore-water pressures and decrease soil strength (Collins and Znidarcic, 2004; Sidle and Ochiai, 2006; Lu and Godt, 2013; Bogaard and Greco, 2016). Therefore, for different antecedent soil moisture conditions, the rainfall events that are needed to trigger landslides are different. For instance, if the antecedent soil moisture is dry, high-intensity rainfall or prolonged rainfall is needed to increase the water in the soil and trigger landslides, in this case, the higher threshold is more appropriate to avoid too many false alarms. However, for antecedent conditions at saturation, even small rainfall could cause the initiation of landslides. Here a lower threshold is required to avoid the missed alarms. In other words, adjusting the landslide warning thresholds according to the antecedent soil moisture conditions could be more effective to reduce the incorrect

84 predictions (e.g. false alarms and missed alarms), benefiting the application of rainfall thresholds in
85 the landslide prediction. Based on this cognition, Ponziani et al. (2012) developed an early warning
86 system with the soil moisture -rainfall thresholds as the tool for the landslide prediction in central Italy.
87 Ciabatta et al. (2016) used the same system for predicting the landslide occurrence under climate-
88 change scenarios. Despite these thresholds are defined considering the antecedent soil moisture
89 conditions, few studies are carried out directly based on the traditional rainfall thresholds (e.g. rainfall
90 intensity-duration (ID) threshold, cumulated event rainfall-rainfall duration (ED) threshold) to improve
91 their prediction performance.

92 Therefore, this study attempts to achieve adjusting the rainfall threshold level according to the
93 antecedent soil moisture conditions, which could directly take advantage of the rainfall thresholds.
94 This problem could be addressed by estimating the landslide occurrence probability given various
95 conditions characterized by the antecedent soil moisture and the severity of the recent rainfall event,
96 after which a critical value is selected to divide these conditions into those that are likely to trigger
97 landslides and unlikely to trigger landslides. Here the soil moisture conditions are estimated by a
98 distributed hydrological model called SHETRAN (Système Hydrologique Européen TRANsport)
99 (Birkinshaw and Ewen, 2000), and the severity of the recent rainfall event is characterized by the
100 cumulated event rainfall-rainfall duration (ED) thresholds with different exceedance probabilities. In
101 this way, we propose a probabilistic threshold which directly integrates the antecedent soil moisture
102 conditions with the ED rainfall thresholds. In order to take into account both conditions with landslides
103 and without landslides, two-dimensional Bayesian analysis is applied to estimate the landsliding
104 probabilities. The receiver operating characteristic (ROC) approach is employed to evaluate the
105 thresholds' prediction performance. For better assessing the proposed threshold, its prediction
106 performance is compared with that of the ED rainfall threshold. The study is carried out in a sub-region
107 of the Emilia-Romagna Region in northern Italy, owing to the abundance of landslide records and
108 hydrometeorological data. The study period is from 2005 to 2015, during which all the required data

are the most complete. The data of the period 2005 to 2013 (as the calibration period) are used to estimate the landslide probabilities of different conditions and define the probabilistic thresholds, while the data of the last two years from 2014 to 2015 (as the validation period) are for the validation of the proposed thresholds.

This paper is organized as follows. Section 2 introduces the study area and sources of data. Section 3 details the characteristics of hydrological model SHETRAN and the approach of determining the thresholds. Section 4 describes the results of the proposed method. Further discussions and limitations of this study are outlined in Section 5, followed by conclusions and outlook in the final section.

2 Study Area and Data

2.1 Study area

The Emilia-Romagna region is located in northern Italy, with a terrain changing from a wide flat area in the north and east to a mountainous area in the south and west. The elevation ranges from 0 m to 2165 m (Fig 1). There is a typical Mediterranean climate in the region, warm and dry in summer, and mild/cold and wet in winter. The average annual rainfall varies a lot across the region, where it has a minimum value of about 500 mm in the foothills, while in the mountains, it can reach 2000 mm.

The mountainous area of the region is extremely subject to landslides (Fig 1), with more than 20% of its territory covered by active or dominant landslide deposits (Berti et al., 2012). Landslides have a high threat to human life and properties, although they do not usually cause causalities, they lead to damage to properties, infrastructures and natural resources. The cost of regeneration and remedial works is high, approximately €130 million during the period 2008 to 2012 for this region (Berti et al., 2012). Additionally, with the development in the mountainous areas, the cost of post-disaster constructions becomes higher and higher due to the increased exposure of people and properties to landslide hazards.

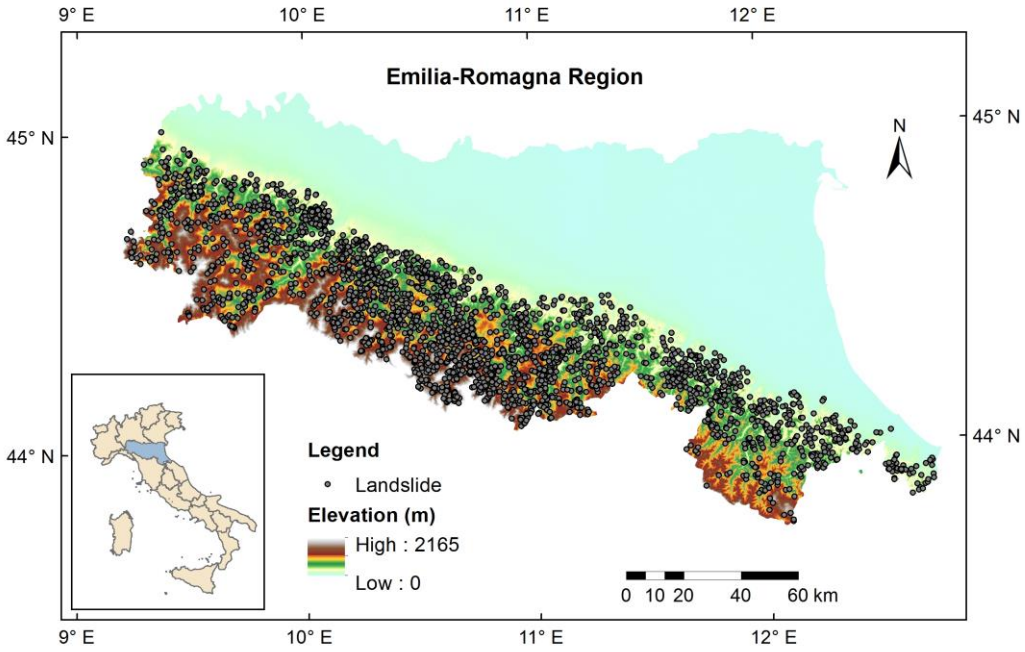

Figure 1. Map of the Emilia-Romagna region and landslides in this region.

Two catchments in the mountainous portions are chosen as the study area (Fig 2), because the data required by this study is relatively complete in these areas. The southern and southwestern sector of the catchments is characterized by hills and mountains, while the northeastern part is the wide plain. These two catchments are mainly covered by trees and crops. Catchment 1 has an area of 1191 km^2, with 11 weather stations operated, as for Catchment 2, its area is 722 km^2 and there are 5 weather stations. The weather stations can provide the daily measurements of precipitation, air temperature and mean wind speed. For both catchments, there is a flow monitoring station at the outlet, measuring the flow data at a daily resolution.

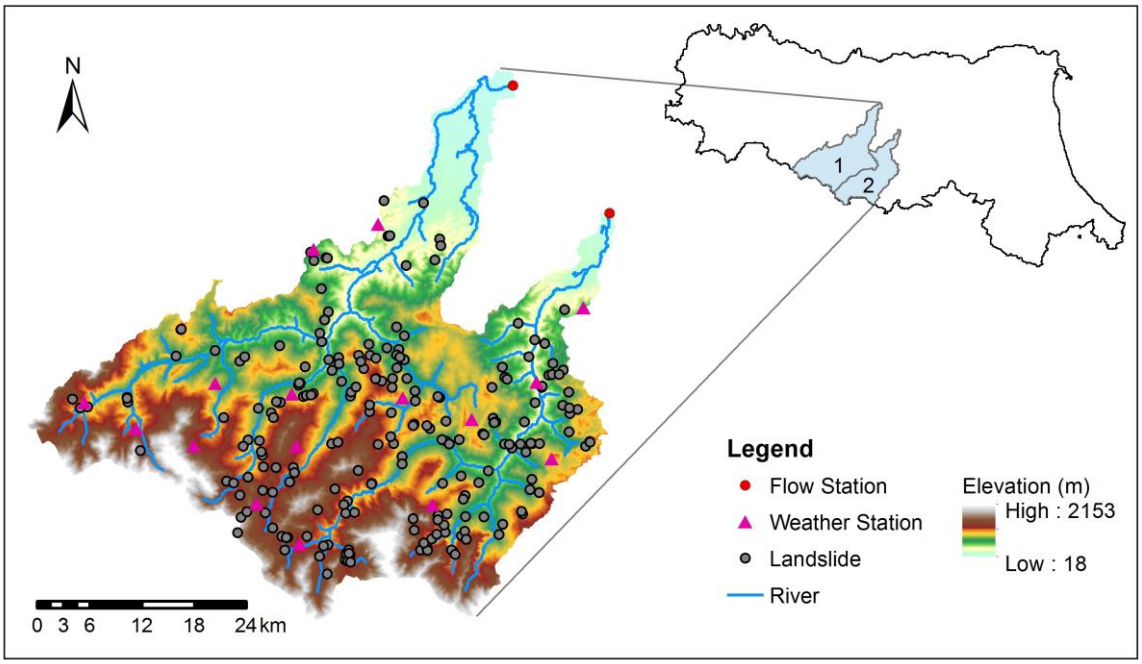

Figure 2. Map of the study area with the terrain elevation and the distribution of weather stations, flow stations and landslides.

2.2 Landslide data

The landslide data adopted in this study is from the Emilia-Romagna Geological Survey, an agency maintaining a catalogue of historical landslides in the Emilia-Romagna region. The landslides since 1900 are recorded in this catalogue, whose information comes from various sources, such as reports to local authorities, national and local press, technical documents. Most landslides that cause casualties and damage are recorded in the catalogue; however, landslides with little damage or influences, especially those occurring in the remote area are likely to be undetected. For each landslide, the catalogue includes the information of its location, date of occurrence, date accuracy, landslide characteristics (length, width, type and material), triggering factors, damage and references. Unfortunately, not all landslides are recorded with the complete information, in most cases, only the location and occurrence date are recorded.

Based on the available information, landslides whose occurrence date is recorded with daily accuracy and weekly accuracy are selected for analysis. The reason for this selection is that landslides with daily

158 accuracy in the study area are limited, not enough for the analysis. To reduce the uncertainties caused
159 by the data with weekly accuracy, we have made some corrections to their date. For each landslide,
160 the recent rainfall event is searched, and its occurrence date is adjusted to the end date of the rainfall
161 event. As a result, a total of 274 landslides are selected over the study period 2005 to 2015 for the
162 study area (Fig 2). There are 239 landslides occurring during the calibration period 2005 to 2013,
163 among which 92 landslides are recorded with daily accuracy and 147 with weekly accuracy. For the
164 35 landslides in the validation period 2014 to 2105, 14 of them have a daily accuracy, with the rest
165 recorded with weekly accuracy.

166 The yearly and monthly distribution of landslide occurrences over the study period 2005 to 2015 is
167 shown in Fig 3 as well as the corresponding rainfall distribution. It can be seen from Fig 3a, the number
168 of yearly landslide occurrences varies a lot from 2 and 64, with an average of around 25 landslides per
169 year. There is no obvious trend of the yearly landslide number over these years. It is expected that this
170 irregular distribution could be explained by the variation of the yearly rainfall, however, although they
171 have the similar distribution for some periods (2005 to 2010), for other years their distribution differs
172 a lot, especially the distinct difference in the year 2011, 2012 and 2014. One possible reason is that the
173 occurrence of landslides is a result of multiple factors, even for the rainfall-triggered landslides, rainfall
174 is not the only factor affecting the slope stabilities. For instance, earthquake, the changes in land use
175 and human activities may alter the slope structure and affect the slope stabilities, changing the
176 possibilities of landslide occurrences. Besides, the landslide data used for analysis are not complete,
177 in which some small landslides are likely to be undetected or neglected. Therefore, there may be some
178 biases of this distribution. Despite this, it is noted that the distribution of yearly landslides in our study
179 area is in line with that in northern Italy, which is shown in the work of Peruccacci et al. (2017). The
180 results in Fig 3b show that the change of monthly landslides is similar with that of monthly rainfall,
181 which increases from January to March and then decreases to July or August, followed by a grow until
182 November. The rainfall presents a decline in December, while the landslide occurrence in December

grows dramatically. This unexpected increase could be due to the extreme rainfall event occurred during 2009-12-23 to 2009-12-25, which caused more than 29 landslides, making a great contribution to the number of December's landslides. It is also found that the majority of landslides occurred during the wet season (October to May), indicating the crucial role of rainfall in the initiation of landslides.

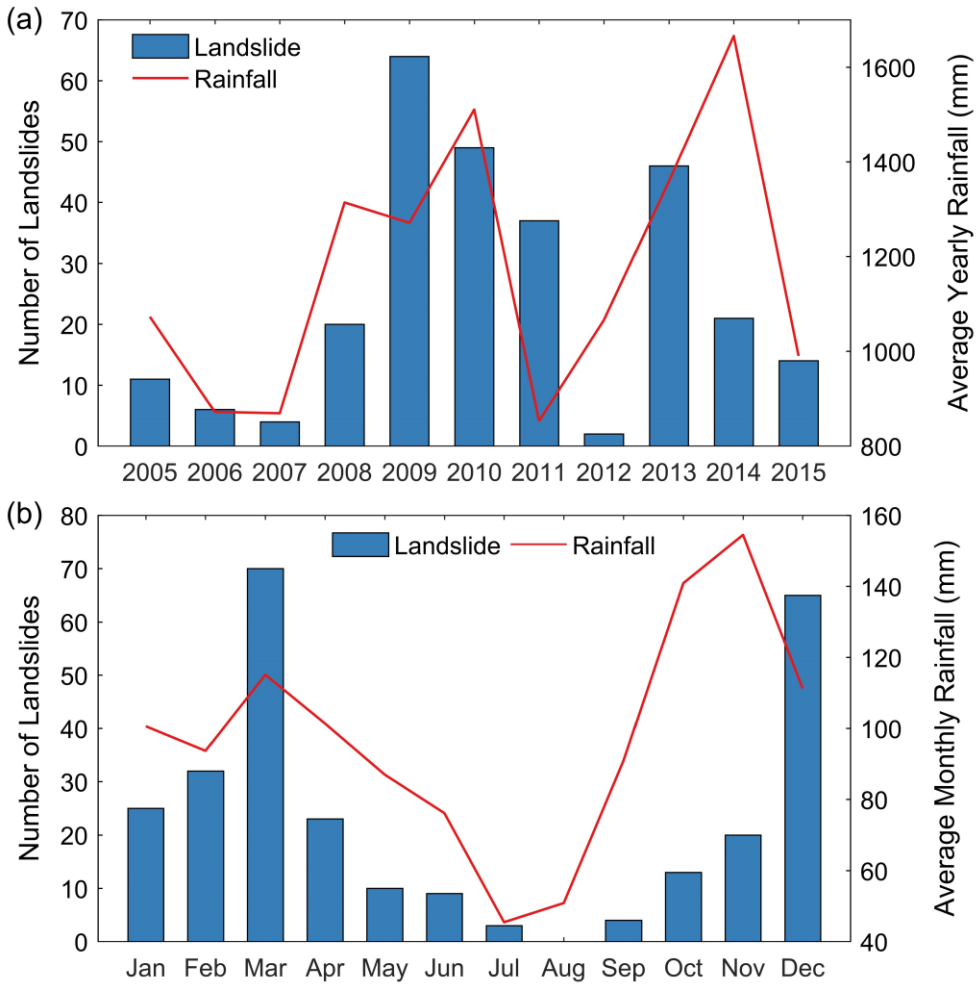

Figure 3. The distribution of landslide occurrence and rainfall over the study period 2005 to 2015, (a) for yearly distribution and (b) for monthly distribution.

2.3 Data for the hydrological simulation

Regional Agency for the Prevention, Environment and Energy of Emilia-Romagna (Arpae) maintains measurements of hydrological and meteorological data in the Emilia-Romagna region. The weather stations distributed in the study area all have tipping-bucket rain gauges, being able to collect rainfall

data at a daily time scale before 2001 and every 30 minutes since 2001. Besides, they also measure other daily meteorological data, like air temperature and wind speed. The flow stations at the outlet of catchments can provide daily flow data. All these data are available online (http://www.smr.arpa.emr.it/dext3r/). In addition to the meteorological data as the driving force for the hydrological model and the flow data used for calibration, some environment features (i.e., DEM, land cover and soil type) are needed to characterize the studied catchments. In this study, the spatial variation of land cover and soil type is not taken into account, therefore only the DEM information is used, which are from the Shuttle Radar Topography Mission (SRTM) 3 Arc-Second Global DEM datasets (90m). Although the rainfall data of every 30 minutes are available over the study period, most of the other required data are at a daily resolution, which restricted the time resolution of this study to be daily. The use of these data for hydrological simulations will be introduced in Section 3.1.

3 Methods

3.1 Soil moisture simulation using the hydrological model

SHETRAN (Système Hydrologique Européen TRANsport) is a distributed hydrological model, originated from the Système Hydrologique Européen (SHE) (Abbott et al., 1986). It is capable of simulating basic processes and pathways for flow and transport in river catchments (Ewen, 1995). SHETRAN has been applied in a wide range of catchments and proved to be a reliable hydrological model (Birkinshaw and Ewen, 2000; Birkinshaw, 2008; Norouzi Banis et al., 2004; Zhang et al., 2013; Zhang and Han, 2017). SHETRAN has three main components: water flow, sediment transport and contaminant transport. This study only takes advantage of the water flow component, which contains major elements of the hydrological cycle, as shown in Table 1. Meteorological inputs to SHETRAN are: precipitation, potential evapotranspiration (measured or calculated) and the heat budgets used to calculate rates of snowmelt. Catchment properties like DEM, soil properties and land use are also requirements. These data are allowed to be spatially distributed, because the physics-based governing

partial differential equations for flow and transport are solved on a three-dimensional grid. The parameters used in this model is listed in Table 2.

Although SHETRAN is able to simulate the hydrological response by taking into account the spatial variation of land cover and soil properties. In this study, only the meteorological information and DEM properties are spatially distributed. We divided the study area into several zones using Thiessen polygons (Croley II and Hartmann, 1985) based on the location of weather stations. The rainfall and evapotranspiration conditions are assumed to be the same within an individual zone, and the corresponding data are assigned. The reason for not considering the spatial variation of land cover and soil type is as follows. Due to the lack of field measurements, the parameters used to characterize the catchment properties need to be calibrated with the observed flow data. If the parameters related with the land cover and soil type are spatialized, too many parameters may cause some problems like overfitting. Besides, through analysing the distribution of land cover and soil type, it is found most areas are characterized by the similar information, for instance, most lands are covered by tree and crop, and soil type is gleyic solonetz. Therefore, we assume the land cover and soil type in the study area are homogeneous and parameters related to them are the same for the whole study area.

Snowmelt is not considered when simulating the hydrological process. The reason is although the meteorological conditions are spatialized, their spatial resolution is still coarse for the consideration of snowmelt, because the snowmelt module in SHETRAN works based on the temperature (whether exceed 0 ℃), and for mountainous areas, the temperature changes with the increase of elevation, the coarse meteorological input may cause the wrong simulation of snowmelt. Besides, the capability of SHETRAN to simulate the snowmelt process has not been explored widely.

Table 1 Equations of hydrological processes in SHETRAN

Processes	Equation
Evaporation	Penman-Monteith equation (or a fraction of potential evaporation rate) (Abbott et al., 1986)

Canopy interception and drip	Rutter equation (Abbott et al., 1986)
Subsurface flow	Variably saturated flow equation (3D) (Parkin, 1996)
Overland flow	Saint-Venant equations, diffusion wave approximation (2D) (Abbott et al., 1986)
Channel flow	Saint-Venant equations, diffusion wave approximation (flow in a network of 1D channels) (Abbott et al., 1986)
Snowpack and melt *	Accumulation equation and energy budget melt equation (or degree-day melt equation) (Abbott et al., 1986)

240 * Snowpack and melt are not considered in this study.

241 Table 2 Parameters used in the hydrological model SHETRAN

	Parameters	Minimum Value	Maximum Value
Vegetation	Canopy storage capacity (mm)	0	-
	Leaf area index	0	-
	Maximum rooting depth (m)	0	20
Soil properties	Saturated water content	0.05	1
	Residual water content	0	0.8
	Saturated conductivity (m/day)	0	-
	Van genuchten-alpha (cm^{-1})	0	-
	Van genuchten-n	1.2	-
	Soil depth (m)	0	-
Others	AE/PE ratio at field capacity	0	-
	Strickler overland flow roughness coefficient ($m^{1/3}$ s^{-1})	0	-

242

243 When calibrating parameters, the difference between the observed and simulated flow is minimized
244 by maximizing the Nash-Sutcliffe Efficiency (NSE) (Nash and Sutcliffe, 1970) which is defined as:

$$R^2 = 1 - \frac{\sum_{i=1}^{n}(Q_i^o - Q_i^m)^2}{\sum_{i=1}^{n}\left(Q_i^o - \overline{Q^o}\right)^2} \quad (1)$$

245

246

where Q_i^o and Q_i^m are the i^{th} observed and simulated streamflow, respectively. $\overline{Q_o}$ is the arithmetic mean of the observed streamflow. n is the total number of days in the calibration period. The optimal value of NSE is 1. The model is calibrated for the period from 2004 to 2013 with the first year as the warm-up period, and then validated for the period from 2014 to 2015. The spatial resolution of our model is 1 km.

Based on the above settings, some problems need to be noted. First, the variation of hydrological response simulated by our model is only related with the meteorological conditions and the topography, therefore, the soil moisture conditions which are concerned in this study are only the result of the meteorological conditions and the topography. Second, the model is only calibrated with flow data at the outlet of the catchment, it is difficult to validate the simulated soil moisture. However, as SHETRAN is physically based, it is considered the model calibrated well is capable of providing a reliable simulation of the hydrological response, including the soil moisture's response to meteorological conditions.

3.2 Definition of rainfall events and rainfall thresholds

Before defining the threshold for landslide occurrences, rainfall events need to be detected. As each grid cell has been assigned a rain gauge during the hydrological simulations (using Thiessen polygons), we only need to reconstruct rainfall events for each rain gauge. In order to make the definition of rainfall events objective and reproducible, we applied the automatic procedure proposed by Melillo et al. (2014) in this study. The algorithm requires an input parameter to define the minimum dry period between two consecutive rainfall periods, and this parameter is allowed to vary with seasonal and climatic conditions. Here we set a dry period of 2 days for the dry season and 4 days for the wet season. The dry season is from June to September, while the wet season is from October to April, this classification is based on a function of the climate and altitude (Peruccacci et al., 2017). Once the rainfall event is constructed, the rainfall conditions associated with landslides are defined, where the

duration D (day) is from the start date of rainfall event to the date of landslide occurrence, and the cumulated event rainfall E (mm) is then calculated by accumulating the rainfall during this period.

With the rainfall conditions associated with landslide occurrences, the ED rainfall threshold is determined using the Frequentist approach proposed by Brunetti et al. (2010). They assumed the general formulation of threshold curves is a power law:

$$E = (\alpha \pm \Delta\alpha) \cdot D^{(\gamma \pm \Delta\gamma)} \quad (2)$$

where α is a scaling constant (the intercept), γ is the shape parameter (defining the slope of the power law curve). Δα and Δγ represent the uncertainties of α and γ, respectively. Thresholds with different exceedance probabilities are calculated and evaluated.

3.3 Bayes' theorem

Two-dimensional Bayesian analysis is used to evaluate the conditional probability of the landslide occurrence given the joint occurrence of two factors. Here the two factors are the antecedent soil moisture conditions and the severity of the recent rainfall event. The antecedent soil moisture conditions are indexed by the simulated soil moisture of the day preceding the rainfall event. Considering the distinct variation ranges of the simulated soil moisture series for different grid cells, in order to make them comparable and used for thresholds definition, the simulated soil moisture here is normalized based on the cumulative probability distribution of its grid cell's long-term soil moisture series (termed as soil wetness). As a result, the value of the soil wetness ranges from 0 to 1, the higher the value, the wetter the soil conditions. According to the value of soil wetness, the soil moisture conditions are classified into five categories ([0,0.2), [0.2,0.4), [0.4,0.6), [0.6,0.8), [0.8,1]). Rainfall events are classified into six categories according to the level of severity, which is characterized by the cumulated event rainfall-rainfall duration (ED) thresholds with different exceedance probabilities. For instance, rainfall events located below the minimum threshold will be classified into one category, indicating the severity is low. Those located between the minimum threshold and the threshold at 5%

exceedance probability (T_5) will be classified into another category. Here are six categories, with different thresholds as the boundary (T_{min}, T_5, T_{10}, T_{20}, T_{50}). As a result, there are 5 × 6 cells for the Bayesian analysis. To make use of as much as possible data, we merge all the data of grid cells with landslides into a dataset, on which the Bayesian analysis is based. A sample of this dataset is shown in Table 3.

Table 3 Sample dataset for the Bayesian analysis

	Rainfall event	Antecedent Soil Wetness	Rainfall duration (day)	Cumulated rainfall (mm)	Landslide
Grid Cell 1	1	0.85	2	3.6	No
	2	0.92	3	45.2	No
	3	0.88	1	10.4	No
	4	0.79	1	2.8	No
	5	0.84	6	29.4	Yes
	…	…	2	11	…
Grid Cell 2	1	0.92	8	43	Yes
	2	0.85	6	24.6	No
	3	0.88	3	65	No
	4	0.79	5	28	No
	5	0.87	8	26.8	No
	…	…	…	…	…
Grid Cell N	…	…	…	…	…

Two-dimensional Bayes' theorem can be expressed as follows:

$$P(A|B,C) = \frac{P(B,C|A) \cdot P(A)}{P(B,C)} \quad (3)$$

where A indicates the event of at least one landslide occurrences. B and C indicate the antecedent soil moisture conditions and the severity of the recent rainfall, respectively. The notation "B, C" means the antecedent soil moisture is within a certain range of values, while the rainfall event has a certain level of severity. In other words, the notation "B, C" represents the condition of one of the 5 × 6 cells mentioned above (hereafter cell condition). $P(B,C|A)$, $P(A)$, $P(B,C)$ and $P(A|B,C)$ can be defined as follows:

$P(B, C|A)$, the conditional probability of "B, C" given A, also known as likelihood. It is the probability of observing a certain cell condition when a landslide occurs.

$P(A)$, the prior probability of A. It is the probability of landslide occurrences regardless of the cell conditions.

$P(B, C)$, the marginal probability of "B, C". It is the probability of observing a certain cell condition regardless of whether a landslide occurs.

$P(A|B, C)$, the conditional probability of A given "B, C", also known as posterior probability. It is the probability of observing at least one landslide when a certain cell condition occurs.

The probabilities are usually calculated in terms of relative frequencies. Thus, these probability terms can be approximated using the following equations:

$$P(A) \approx \frac{N_A}{N_R} \tag{4}$$

$$P(B, C) \approx \frac{N_{B,C}}{N_R} \tag{5}$$

$$P(B, C|A) \approx \frac{N_{(B,C|A)}}{N_A} \tag{6}$$

where:

N_A, the total number of landslide occurrence events, those landslides that occurred during the same time at the same grid cell are considered as one event and counted once.

N_R, the total events of all cell conditions over the calibration period.

$N_{B,C}$, the number of events which belong to one certain cell condition.

$N_{(B,C|A)}$, the number of events which have triggered landslides while belong to one certain cell condition.

After estimating the probability of landslide occurrences given the different cell conditions, the thresholds can be determined by comparing the probability values with a critical value. For instance, if 0.001 is chosen as the critical value, for each soil moisture category, the categorie of rainfall events can be separated by determining whether their probabilities exceed 0.001. In this way, the rainfall thresholds could be determined for different soil moisture conditions. The critical value will be selected by evaluating the prediction performance of the threshold it determined.

3.4 The validation of thresholds

The thresholds are validated with the help of the contingency matrix (Table 4) and Receiver Operating Characteristic (ROC) curves. This is the most common manner used in landslide prediction studies (Staley et al., 2013; Gariano et al., 2015; Mirus et al., 2018). The contingency matrix includes four components: Ture Positive (TP), False Negative (FN), False Positive (FP) and True Negative (TN), which are four possible outcomes of the thresholds' prediction results. TP means the threshold predicts landslide occurrences successfully; FN is an error where the thresholds doesn't predict the occurrence of landslides; however, in reality landslides occur; FP is an error where the threshold predicts the occurrence of landslides; however, there are no landslide occurrences in reality; TN means the threshold correctly predicts the non-occurrence of landslides. ROC analysis is based on the contingency matrix, where two skill scores are calculated: Hit Rate (HR) and False Alarm Rate (FAR).

Hit Rate (HR) is also known as the true positive rate, used to measure the proportion of landslides that are correctly predicted:

$$HR = \frac{TP}{TP + FN} \tag{7}$$

False Alarm Rate (FAR) is also known as the false positive rate, used to measure the proportion of false alarms over the events when no landslide occurs:

$$FAR = \frac{FP}{FP + TN} \quad (8)$$

The value of HR and FAR ranges between 0 and 1. When HR equals to 1 and FAR equals to 0, the optimal performance is achieved (the perfect point). For better evaluating the threshold, the Euclidean distance (d) to the perfect point is also calculated for each threshold scenario (Gariano et al., 2015). The smaller the distance, the better the prediction ability.

Table 4. The Contingency Matrix

Predicted \ Observed	Yes	No
Yes	TP	FP
No	FN	TN

4 Results

4.1 Soil moisture estimated by the hydrological model

The hydrological model is calibrated with the flow data for the period 2004 to 2013, with the first year as the warm-up period. The optimal performance is achieved when NSE equals to 0.82 for Catchment 1 and 0.80 for Catchment 2. For the purpose of validation, the calibrated parameters are used to simulate the hydrological process for the period 2014 to 2015, whose NSE value is 0.76 for both catchments. Although the value of NSE is not very high, it is regarded as acceptable, indicating the calibrated model is feasible to simulate the hydrological response to meteorological conditions. The top soil depth is calibrated as 0.28m for both catchments, therefore, the soil moisture simulated by the hydrological model refers to the water content in the upper soil layer with the depth as 0.28m. In order to better demonstrate the characteristics of the simulated soil moisture, its spatial variation and temporal evolution are introduced.

Three periods are chosen as examples to introduce the spatial distribution of the soil moisture data, as shown in Fig 4. Period 1 is the representative of dry periods. Period 2 is selected to represent the periods with intense rainfall, whose antecedent periods are relatively dry. Period 3 is an example of the periods during which the rainfall is intense, and there is intense rainfall preceding these periods. The soil moisture value presented in Fig 4b is the value of the period's last day. There is a similar pattern in the soil moisture distribution of these three periods. The grid cells close to the river are wetter than others, and the grid cells in the north have a higher value compared with those in the south if grid cells near the river are not taken into account. This distribution pattern can be explained by the topography, where the southern area of the catchment is characterized by hills and mountains, and the northern area is flat. Although the soil moisture distribution is influenced by multiple factors, like topography, landcover, soil type, meteorological conditions and water routing processes, the difference of landcover and soil type was not distinguished when conducting hydrological simulations. Therefore, in this study the topography is the main factor that may affect the soil moisture distribution. Therefore, it is considered the spatial distribution of soil moisture displayed in Fig 4b is reasonable.

There is no rainfall in Period 1 and it has the lowest soil moisture values. Although the rainfall of Period 2 is intenser than Period 3, its soil moisture values are lower than those of Period 3. The reason for this is that there is continuous rainfall before Period 3 (as shown in Fig 4a). This phenomenon demonstrates that the simulated soil moisture has a good response to the rainfall conditions, which is in line with the physical process.

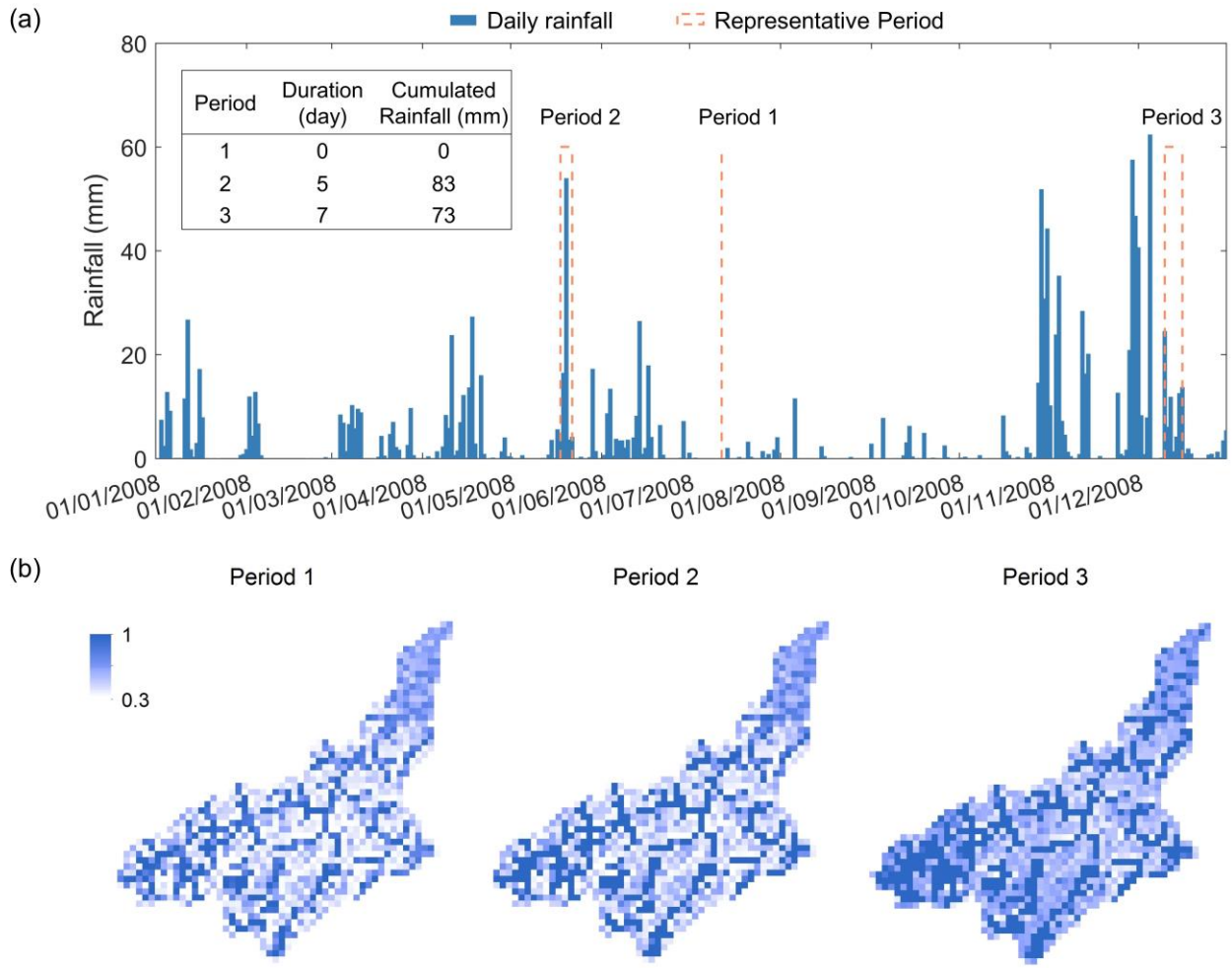

Figure 4. The spatial distribution of the soil moisture data estimated by SHETRAN. (a) The rainfall series for the year of 2008 and the rainfall information of three representative periods used for the analysis. (b) The spatial distribution of the soil moisture data of three representative periods for Catchment 1 with 1 km resolution.

Six grid cells that have more landslides are selected to further study the statistical distribution of soil moisture data over the calibration period. Figure 5a shows the location of these six representative grid cells, and the cumulative probabilities of their soil moisture data are plotted in Fig 5b. The cumulative probability distribution of these six grid cells differs a lot. For Grid Cell 1 and Grid Cell 2 close to the river, they have high soil moisture values, specifically, their soil moisture is almost saturated for the most time. For Grid Cell 3 and Grid Cell 4, their soil moisture values vary within a larger range, indicating they are more sensitive to the change of meteorological conditions. The soil moisture for

Grid Cell 5 and Grid Cell 6 is always at a low level, with a smaller variation range. The difference in the distribution is mainly caused by their different topographies. Due to the difference of the soil moisture variations, we use the cumulative probability to represent the real soil moisture value for the purpose of comparability. The circle in Fig 5b represents the antecedent soil moisture conditions of landslides. It is found that the antecedent soil moisture conditions vary a lot, changing from 0.1 to 1. One possible reason is that the antecedent period differs a lot, which is dependent on the duration of the rainfall event. For instance, if the rainfall event has a duration of 10 days, the soil moisture before this event is likely to be dry. In this case, the occurrence of the landslide is mostly contributed to the rainfall event and has little relation with the antecedent soil moisture.

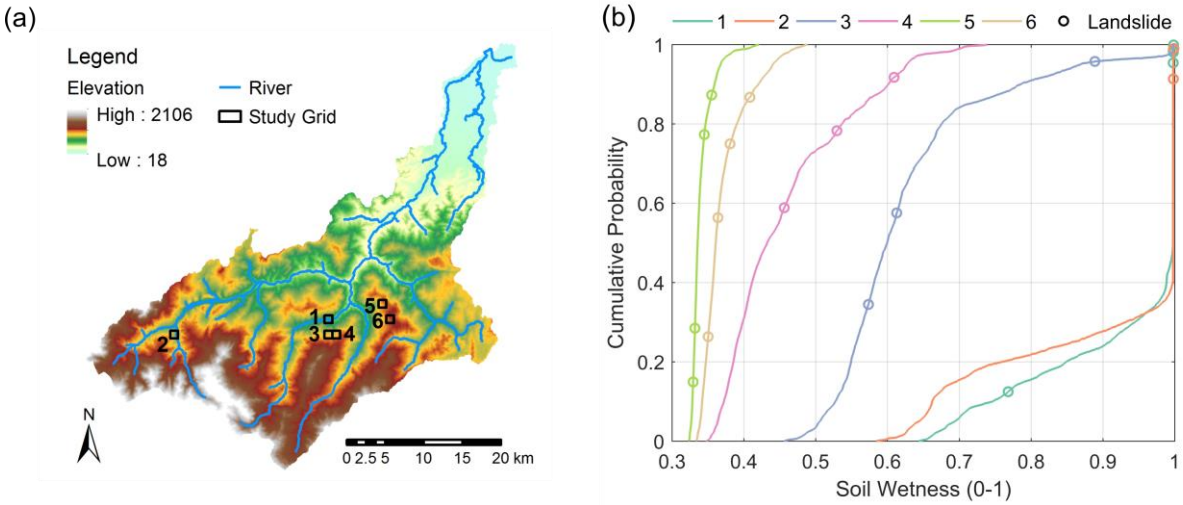

Figure 5. The statistical distribution of soil moisture data over the calibration period 2005 to 2013. (a) The location of six representative grid cells used for the analysis. (b) The distribution of cumulative probabilities of soil moisture data for six representative grid cells and their landslides.

4.2 Rainfall thresholds

Applying the automatic procedure of defining rainfall events to all rain gauges in the study area, 212 rainfall events were identified for the landslide occurrences. Two variables (cumulated event rainfall and rainfall duration) of these events are calculated for the determination of ED rainfall thresholds. The rainfall threshold with different exceedance probabilities (5%, 10%, 20% and 50%) as well as the

minimum rainfall threshold for landslide occurrences are shown in Fig 6. The minimum threshold here is the threshold defined without considering the exceedance probability. The national threshold of Italy at 5% exceedance probability proposed by Peruccacci et al. (2017) is also shown in Fig 6. Its equation is $E = 26.59 \cdot D^{0.39}$ with duration in days, which is transferred from the equation $E = 7.7 \cdot D^{0.39}$ with duration in hours. It is interesting to find that the national threshold is very similar to our defined threshold at 50% exceedance probability. The rainfall events associated with landslides have a great variation for both variables, with the duration in the range of $1\,day \leq D \leq 46\,days$, and the cumulated event rainfall in the range of $5.2mm \leq E \leq 747.6mm$. For the thresholds defined using the Frequentist approach proposed by Brunetti et al. (2010), taking the exceedance probabilities of 5% as an example, as expected, there are 10 pairs of the (D, E) data (5% of 212 rainfall conditions) below the P5 threshold.

The uncertainties associated with the parameters of the ED thresholds are listed in Table 5. It is clear that parameters of the thresholds defined in this study have much higher relative uncertainties (Δα/α and Δγ/γ) than the national threshold, indicating that our defined thresholds are more sensitive to the addition of new rainfall events with landslides. The higher uncertainties could be caused by the small sample size used for the threshold definition, as explored by Peruccacci et al. (2012) and Gariano et al. (2015). The relative uncertainty Δα/α of our defined thresholds decreases with the increase of the exceedance probability, reaching 12.47% at 50% exceedance probability. As the distribution of the empirical data also has an impact on the uncertainties, the lower relative uncertainty of 50% exceedance probability may benefit from the distribution of the data.

Table 5 Parameters of ED thresholds and the related uncertainties and relative uncertainties

Label	Region	Probability	α	Δα	Δα/α	γ	Δγ	Δγ/γ
T_{50}	Studied Area	50	31.28	3.9	12.47%	0.42	0.041	9.76%
T_{20}	Studied Area	20	17.42	2.35	13.49%	0.42	0.041	9.76%
T_{10}	Studied Area	10	12.84	1.83	14.25%	0.42	0.041	9.76%
T_{5}	Studied Area	5	9.97	1.5	15.05%	0.42	0.041	9.76%

T_{min}	Studied Area	0	2.07	0.44	21.26%	0.42	0.041	9.76%
T_{Italy}	Italy	5	26.59	1.04	3.91%	0.39	0.009	2.31%

435

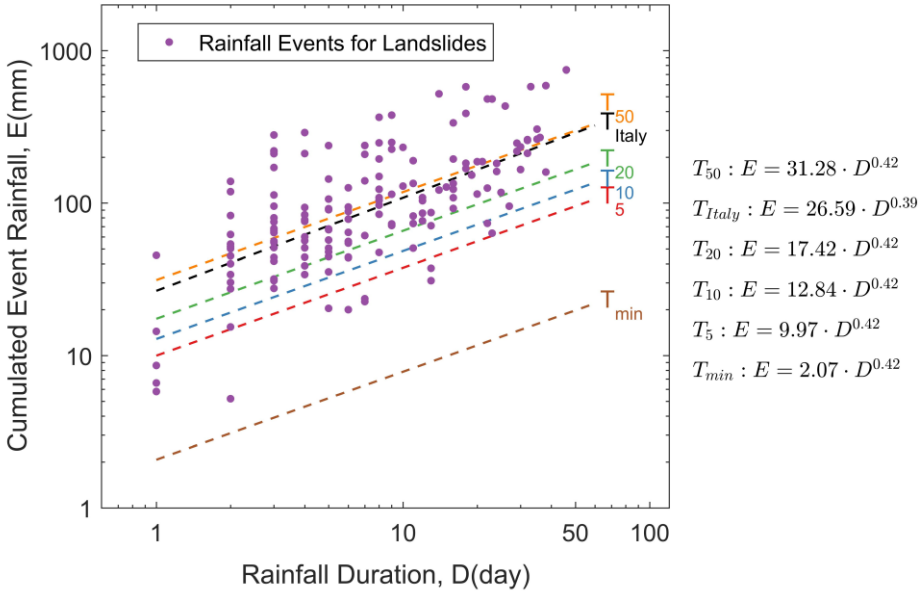

436

437 Figure 6. The rainfall thresholds with exceedance probabilities of 5%, 10%, 20% and 50% (T_5, T_{10},
438 T_{20}, T_{50}) and the rainfall threshold without considering the exceedance probability (T_{min}) for the
439 study area as well as the national threshold of Italy (T_{Italy}) proposed by Peruccacci et al. (2017).

440 **4.3 Probabilistic thresholds**

441 The Bayesian analysis is carried out to the study area following the procedure described in Section 3.3.
442 There are 212 grid cells with landslides among the total grid cells of 1858 for two catchments. During
443 the calibration period, the total rainfall events for the grid cells with landslides are 48927, about 26
444 rainfall events for each grid cell per year. There are 228 events identified for the 239 landslides, with
445 some landslides occurred at the same grid cell on the same day. The results of Bayesian analysis are
446 shown in Fig 7. It is clear the probability of landslide occurrences increases with the severity of the
447 event for both antecedent soil moisture condition and rainfall condition. The maximum probability
448 value of 0.078 is reached when the soil moisture condition and rainfall condition are located in the
449 severest category. There are some unexpected distributions. For instance, for the soil wetness within

the range [0.6,0.8), the rainfall distributed between T_{10} (threshold at 10% exceedance) and T_{20} has the higher probabilities than those distributed between T_{20} and T_{50}. The similar phenomenon can be found for the soil wetness in the range [0.8,1], where the probability is higher for rainfall events located within T_5 and T_{10} than those located between T_{10} and T_{20}. This unexcepted distribution could be due to two factors. The incompleteness of landslides may cause the bias of this distribution, especially for grid cells with few data, even a small variation on the number of landslide occurrences will lead to a different probability value. Besides, the definition of rainfall events responsible for landslide occurrences may have impacts on the distribution. When defining the rainfall events for landslides, its end date is the date of the landslide occurrence rather than the end date of rainfall, which may result in some biases for the two variables of the rainfall event, and thus affect the probability distribution. It is also noted due to these factors, the calculated probability values in Fig 7 are just a proxy of the true probability of landslide occurrence. Despite this, we can make use of this probability distribution to determine the likelihood of landslide occurrences by comparing their probability values.

It is interesting to find that for different antecedent soil moisture conditions, the rainfall events that are likely to trigger landslides differ a lot. For example, for the dry soil conditions (soil wetness < 0.4), the rainfall events with the lower severity level are unlikely to trigger landslides, with the probability of zero. However, when the soil moisture conditions are wet (soil wetness $\geqslant$0.8), even the small rainfall events are likely to trigger landslides. This phenomenon indicates it is necessary to integrate the antecedent soil moisture with the rainfall thresholds, which is the interest of our study.

To define the probabilistic thresholds which integrate the antecedent soil moisture conditions with the rainfall thresholds, different critical values are chosen to determinate the separation between conditions that are likely to trigger landslides and those that are unlikely to trigger landslides. Here 0.001, 0.002, 0.005 and 0.01 are tested, whose results are shown in Table 6. The symbol T_∞ in Table 6 means the threshold is large enough to be exceeded. In this case, landside occurrences are never predicted. The result of the critical value as 0.001 is also presented by the black dashed line in Fig 7. Taking this case

as an example, when the antecedent soil moisture is within [0,0.2), the rainfall threshold T_{20} is chosen as the threshold for the landslide warning. The conditions of other categories are similar. From Table 6, it is found the higher the critical value, the higher the rainfall threshold for the same soil moisture category. To choose a suitable critical value, the prediction performance of these thresholds is evaluated in Section 4.4.

Table 6 The probabilistic thresholds determined by different probability threshold values

Antecedent soil wetness	Rainfall threshold			
	P>0.001	P>0.002	P>0.005	P>0.01
0-0.2	T_{20}	T_{50}	T_{∞}	T_{∞}
0.2-0.4	T_{20}	T_{50}	T_{50}	T_{∞}
0.4-0.6	T_{10}	T_{20}	T_{50}	T_{50}
0.6-0.8	T_{5}	T_{10}	T_{10}	T_{50}
0.8-1	T_{min}	T_{5}	T_{5}	T_{20}

* T_{∞} means the threshold is large enough to be exceeded.

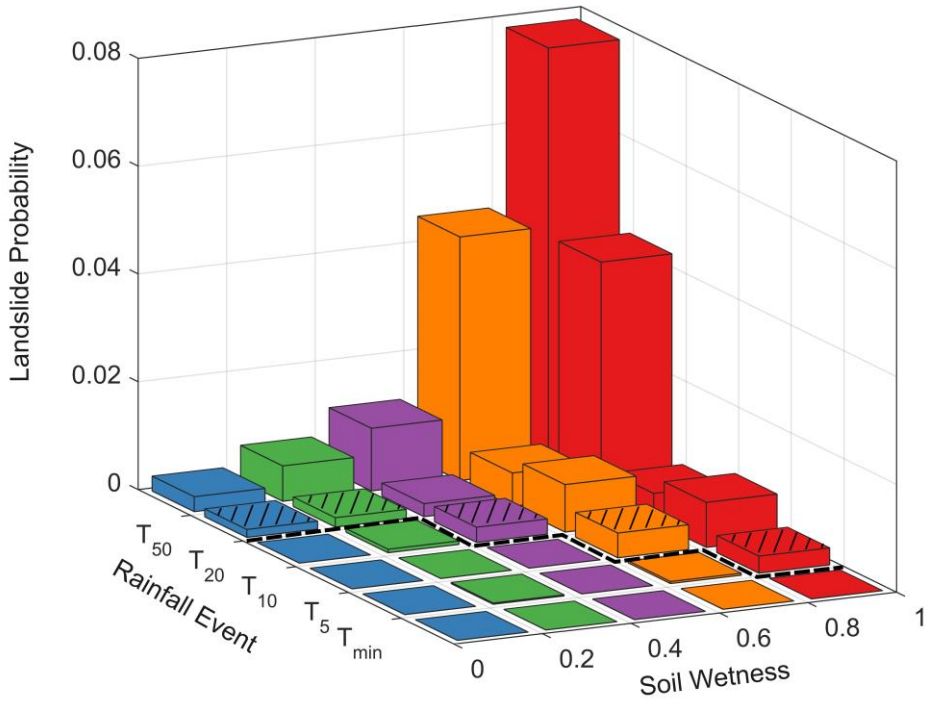

Figure 7. The distribution of landslide occurrence probability based on the two-dimensional Bayesian analysis. The dashed black line is the probabilistic threshold determined by the critical value as 0.001.

4.4 Validation of thresholds

The data of the period 2014 to 2015 are used to validate different thresholds. Here are 11053 events in total, among which 28 events are associated with landslides. ROC curves for different thresholds are plotted in Fig 8. Their prediction results in terms of TP, FN, FP, FN, hit rate (HR), false alarm rate (FAR) and the Euclidean distance (d) are also listed in Table 7. In Fig 8, each point corresponds to one threshold scenario. It can be seen for both rainfall thresholds and probabilistic thresholds, the increment of the threshold will reduce the false alarm rate, sometimes at the expense of decreasing the hit rate. It is interesting to see that the minimum rainfall threshold has a false alarm rate near to 1, which means almost each rainfall event are predicted to trigger landslides. This is the reason why the minimum threshold can't be used directly for the landslide predictions. Although using higher threshold like T_{10} could reduce the false alarms, it is found there is still room to reduce the false alarms without decreasing the hit rate, like the probabilistic thresholds with 0.002 and 0.005 as the critical value. This improvement demonstrates the advantages of integrating the antecedent soil moisture conditions with the rainfall thresholds.

To determine the optimal threshold that meets a balance between the hit rate and the false alarm rate, the Euclidean distance of various thresholds is compared. It is found that the probabilistic threshold has the smallest distance when the 0.01 chosen as the critical value, with hit rate as 0.75 and false alarm rate as 0.11. For ED rainfall threshold, the smallest distance is achieved for T_{20} threshold, whose hit rate is 0.96 and false alarm rate is 0.43. Considering the danger of missed alarms, the hit rate is restricted to the optimal value of 1. In this case, the probabilistic threshold has the optimal performance when the critical value is 0.005, with a false alarm rate as 0.28. The rainfall threshold has the optimal

performance for the T_{10} threshold, whose false alarm rate is 0.58. It is clear that for these two types of the optimal threshold, the probabilistic threshold could provide better prediction performance than the ED rainfall threshold. For the probabilistic threshold, we choose the value of 0.005 as the critical value, because its distance to the perfect point is very similar to that of 0.01, while its hit rate equals to 1.

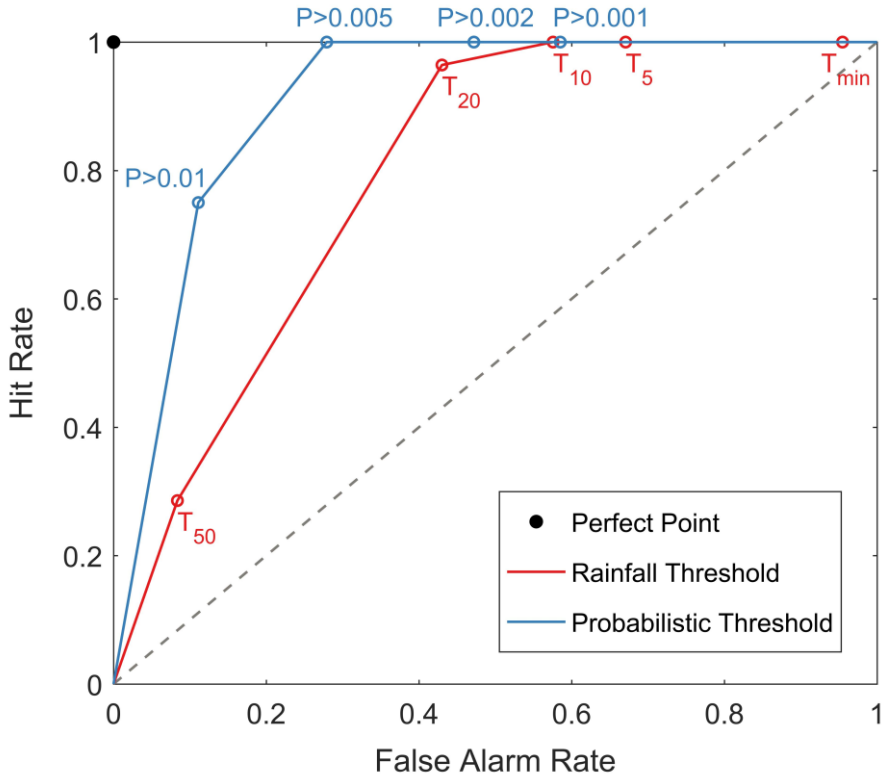

Figure 8. Receiver operator characteristic (ROC) curves for the rainfall thresholds and probabilistic thresholds. Each FAR-HR pair (the point) corresponds to a threshold scenario.

Table 7 The prediction results for various thresholds in terms of TN, FN, FP, TN, Hit Rate(HR), False Alarm Rate(FAR) and the Euclidean distance (d) with the optimal results highlighted

Threshold		TP	FN	FP	TN	HR	FAR	d
Rainfall threshold	T_{min}	28	0	10526	499	1.00	0.95	0.95
	T_5	28	0	7394	3631	1.00	0.67	0.67
	T_{10}	**28**	**0**	**6346**	**4679**	**1.00**	**0.58**	**0.58**
	T_{20}	**27**	**1**	**4742**	**6283**	**0.96**	**0.43**	**0.43**
	T_{50}	8	20	922	10103	0.29	0.08	0.72
Probabilistic threshold	P>0.001	28	0	6451	4574	1.00	0.59	0.59
	P>0.002	28	0	5203	5822	1.00	0.47	0.47

	P>0.005	**28**	**0**	**3078**	**7947**	**1.00**	**0.28**	**0.28**
	P>0.01	**21**	**7**	**1224**	**9801**	**0.75**	**0.11**	**0.27**

5 Discussion

Rainfall thresholds are widely used to predict the landslide occurrence, like the ID threshold and ED threshold. Thresholds with different exceedance probabilities are evaluated to define an appropriate one for the landslide prediction, which could achieve the balance between the correct predictions and incorrect predictions. Once the appropriate threshold is determined, it remains the same regardless of the antecedent soil moisture conditions. However, it is considered that different warning thresholds should be adopted according to the antecedent soil moisture conditions. In this way, the missed alarms and false alarms could be reduced more effectively. Therefore, we propose the probabilistic thresholds which could integrate the antecedent soil moisture conditions with the ED rainfall thresholds. In order to take into account the conditions with landslides and without landslides, the two-dimensional Bayesian analysis is employed. In this study, the antecedent soil moisture condition is the condition preceding the rainfall event that is responsible for landslides, due to the variations of these events' duration, the antecedent period varies. The reason of not using a fix rainfall duration like some reported works (Scheevel et al., 2017; Mirus et al., 2018) is that this study aims to propose a method to improve the performance of the ED rainfall threshold, so the definition of rainfall events remains the same. The results show that the probabilistic thresholds could provide better prediction capabilities especially in term of reducing the false alarm rate, compared with the ED rainfall thresholds. Although we use the simulated soil moisture from hydrological model to index the antecedent soil moisture condition, it can be estimated in other ways, like in-situ measurements, remote sensing products and some indexes of the soil moisture conditions. Therefore, the proposed method could be widely used to take advantage of the soil moisture information to improve the prediction capability of the ED rainfall threshold. Once the probabilistic threshold is determined using the historical dataset, it can be used to predict landslides. Specifically, based on the estimation of the current soil moisture condition, an appropriate rainfall

threshold could be selected, and then through comparing the forecast rainfall with the rainfall threshold, a corresponding prediction could be made.

Despite the advantages of the proposed thresholds, several limitations of this work need to be noted. First, there are problems with the soil moisture estimated by the hydrological model. Although the hydrological model used in this study is a spatially distributed model, we only consider the spatial variation of the meteorological conditions and the topography properties. As a result, the variation of the simulated soil moisture is just due to these two factors. Therefore, the simulated soil moisture can only be considered as an index of the soil moisture conditions instead of the real value of the soil water content. Additionally, in order to make the soil moisture of different locations comparable, the simulated soil moisture data are normalized based on the cumulative probability distribution of its grid cell's long-term simulated data (termed as soil wetness). In this way, the soil wetness could represent the relative soil moisture conditions based on its location and can be used to define the threshold due to the same variation range. Another problem concerns the effectiveness of the hydrological model, since the hydrological model is only calibrated with the flow data at the outlet of the catchment. The lack of the calibration of the simulated soil moisture is really a limitation of this study, however, the simulated soil moisture is regarded as useful for several reasons. First, as the hydrological model is physically based, the calibrated model could be considered effective to simulate the hydrological response including the soil moisture variations. Second, using the calibrated model, the soil moisture is simulated based on the same mechanism. As a result, for the same location, the soil moisture evolution is solely dependent on the meteorological inputs. In other words, it is feasible to represent the total effect of antecedent meteorological conditions, which is the concern of landslide occurrences. In addition to the temporal variations caused by the meteorological conditions, the simulated soil moisture could also reflect the effect of topography, since the hydrological simulation considers the properties of topography. Besides these two reasons, the spatial and temporal distribution of the

simulated soil moisture has been proved reasonable in Section 3.1. Therefore, we think the soil moisture data used in this study is effective.

Another limitation is about the landslide data used in this study. In order to make use of soil moisture with high resolution, the hydrological model is employed, which limits the study area and reduces the landslide data. Due to the landslide data with daily accuracy in the study area are limited, the dataset extends to those with weekly accuracy. For the landslide with weekly accuracy, we searched for its recent rainfall event and adjusted its occurrence date to the end date of the rainfall event. Although this procedure relates the landslide occurrence to the rainfall event, it also leads to some issues. Assuming the end date of the rainfall event is the occurrence date of landslides could result in longer duration and higher cumulated rainfall of the rainfall event with landslides. The overestimation of the rainfall events in several cases may have an impact on the proposed threshold. Specifically, for the 5×6 cells in Fig 7, the overestimated rainfall events would be shifted to the cells with a lower level in terms of the rainfall severity. According to the Bayes' theorem expressed in Equation 3, this shift would increase the landslide probability of the cells with a lower level of the rainfall severity. Thus, the probabilistic threshold could shift downwards the axis of the rainfall event. In other words, using the landslides with weekly accuracy may cause the overestimation of the proposed threshold, which could lead to an overestimation of the missed alarms. Besides, the dataset used for analysis doesn't include all the landslide occurrences. Some remote landslides or landslides with few casualties or damage are likely to be neglected. This problem could also cause some biases to the results, as analyzed above. The lack of information also has an influence on the validation of the thresholds, which has been highlighted in the work of Gariano et al. (2015). As the Bayesian analysis relies on the previous knowledge, only when the historical data used for the analysis have the representativeness for the future period, the results of Bayesian analysis can be used for landslide predictions. For instance, if the frequency of landslides is affected by changes in land use, land cover, rainfall patterns, etc., the conditions that triggered landslides may not be representative for the future. In this case, the prior probability has

589 changed, and the Bayesian probability based on the previous prior probability may be no longer
590 significant. Therefore, when using the Bayesian analysis, it is important to use the long-term dataset
591 to improve the representativeness of the historical data.

592 In addition to these limitations, some points deserve further discussions. When using the 2-dimensional
593 Bayesian analysis, the antecedent soil moisture conditions are classified into 5 categories, while the
594 rainfall evens are classified into 6 categories. As a result, there are 5×6 cell conditions, on which the
595 Bayesian analysis is based. This classification is a compromise between the number in each cell and
596 the resolution of each factor. If there are sufficient data, more detailed classification could be
597 considered and more detailed results could be concluded.

598 For the purpose of comparison, the cumulated event rainfall- rainfall duration (ED) thresholds are also
599 defined in this study. Considering the rainfall threshold is affected by the number and distribution of
600 the empirical data, we compare the ED thresholds defined in this study with the national threshold of
601 Italy defined by Peruccacci et al. (2017), it is interesting to see the ED thresholds at 50% exceedance
602 probability defined in this study are very similar to the national threshold. Although there are studies
603 proposing the rainfall thresholds in the Emilia-Romagna region (Berti et al., 2012; Martelloni et al.,
604 2012; Lagomarsino et al., 2013; 2015; Segoni et al., 2015), we didn't take them into consideration for
605 two reasons. First, these thresholds are defined using different variables, some of them are not
606 comparable. Second, we define the ED rainfall thresholds with different exceedance probabilities,
607 which are representative of different levels of the thresholds. Therefore, when evaluating the prediction
608 performance, the proposed probabilistic thresholds are only compared with the ED rainfall thresholds
609 defined in this study. It is found the probabilistic thresholds could improve the prediction capabilities.
610 However, this result needs more explorations to test, because the landslide occurrence events during
611 the validation period are very limited. The reason of not using a longer period for the validation is that
612 the calibration procedure which is based on the Bayes theorem requires as many as possible data for
613 the analysis, restricting the length of the validation period. Considering the published works also use

a validation period varying from one year to three years (Martelloni et al., 2012; Segoni et al., 2014; Gariano et al., 2015), we use the data of last two years for the validation purpose. Although the cross-validation approach is a way to improve the reliability of the results, the soil moisture data are simulated by the hydrological model, which are based on the continuous process. As a result, if the leave-one-out cross-validation approach is used, the intermittent data would cause modelling difficulties. Concerning the validation of thresholds, the optimal thresholds are defined only considering the optimization of the skill scores, however, in practice, this procedure should depend on the vulnerability and value of exposed properties and infrastructures.

Finally, our study is carried out at a daily time scale owing to the restriction of data. This may lead to some biases to the characteristics of rainfall events associated with landslides, thus affect the results of the Bayesian analysis, because for shallow landslides, they are typically initiated by intense rainfall. Sometimes an intense rainfall over several hours may trigger landslides by punctuating the saturation. In this case, using daily rainfall to characterize the rainfall event may overestimate the rainfall severity. If applied to the landslide predictions, it will cause the delay of warning.

6 Conclusions

In this study, a probabilistic threshold is proposed for a sub-region of the Emilia-Romagna region in northern Italy. In order to take into account the conditions with landslides and without landslides, the two-dimensional Bayesian analysis is applied to estimate the landslide occurrence probability given the various combinations by two factors. One is the soil moisture conditions preceding the rainfall event, in this study, the soil moisture is estimated using the distributed hydrological model SHETRAN. Another is the severity of rainfall event characterized by cumulated even rainfall-rainfall duration (ED) thresholds with different exceedance probabilities. The soil moisture conditions are classified into 5 categories and the rainfall events are classified into 6 categories. Based on the 5×6 cell conditions, the landslide probabilities are estimated with the data of the calibration period 2005 to 2013. A critical

value is then selected to divide these cells into conditions that are likely to trigger landslides and those that are unlikely to trigger landslides, in this way, a probabilistic threshold is defined. In order to determine an appropriate critical value, probabilistic thresholds defined with different critical values are evaluated by comparing their prediction performances for the data of the validation period 2014 to 2015. The prediction performance is assessed with the receiver operating characteristic (ROC) approach, results show that the optimal probabilistic threshold is reached when using the critical value as 0.005, with the hit rate as 1 and the false alarm rate as 0.28. Besides, through comparing the prediction results with that of the ED rainfall threshold, the proposed probabilistic threshold provides a distinct improvement in terms of reducing the false alarm rate from 0.58 to 0.28. The results demonstrate that adjusting the rainfall threshold level according to the antecedent soil moisture conditions could improve the prediction capabilities of the ED rainfall threshold, indicating the importance of the antecedent soil moisture in the landslide occurrences.

This study provides an effective approach to improve the prediction performance of the ED rainfall threshold, benefiting its application in the landslide prediction. Although the antecedent soil moisture condition is estimated by the hydrological model in this study, it can be estimated in various ways, therefore, the proposed method could be widely applied to take advantage of the soil moisture information to improve the rainfall threshold's performance. More explorations are encouraged to test the performance of our proposed methods.

Acknowledgements

The authors acknowledge Dr. Matteo Berti for providing landslides data and Arpae Emilia-Romagna organization for providing the meteorological data and flow data. The authors also acknowledge Dr. Stephen Birkinshaw from the University of Newcastle for the help with SHETRAN in this study. The first author would like to thank the China Scholarship Council for funding her study at the University of Bristol. This study is supported by the Fundamental Research Funds for the Central Universities of

China (2016B42014) and Resilient Economy and Society by Integrated SysTems modelling (RESIST) (Newton Fund via Natural Environment Research Council (NERC) and Economic and Social Research Council (ESRC) (NE/N012143/1)).

Reference

Abbott, M., Bathurst, J., Cunge, J., O'connell, P., Rasmussen, J., 1986. An introduction to the European Hydrological System—Systeme Hydrologique Europeen,"SHE", 2: Structure of a physically-based, distributed modelling system. Journal of hydrology, 87(1-2): 61-77.

Berti, M. et al., 2012. Probabilistic rainfall thresholds for landslide occurrence using a Bayesian approach. Journal of Geophysical Research: Earth Surface, 117(F4): n/a-n/a. DOI:10.1029/2012jf002367

Birkinshaw, S.J., 2008. Physically-based modelling of double-peak discharge responses at Slapton Wood catchment. Hydrological Processes, 22(10): 1419-1430. DOI:10.1002/hyp.6694

Birkinshaw, S.J., Ewen, J., 2000. Nitrogen transformation component for SHETRAN catchment nitrate transport modelling. Journal of hydrology, 230(1-2): 1-17.

Bogaard, T.A., Greco, R., 2016. Landslide hydrology: from hydrology to pore pressure. Wiley Interdisciplinary Reviews: Water, 3(3): 439-459.

Brunetti, M. et al., 2010. Rainfall thresholds for the possible occurrence of landslides in Italy. Natural Hazards and Earth System Sciences, 10(3): 447-458.

Caine, N., 1980. The rainfall intensity-duration control of shallow landslides and debris flows. Geografiska annaler: series A, physical geography, 62(1-2): 23-27.

Chleborad, A.F., Baum, R.L., Godt, J.W., Powers, P.S., 2008. A prototype system for forecasting landslides in the Seattle, Washington, area. Reviews in Engineering Geology, 20: 103-120. DOI:10.1130/2008.4020(06)

685 Ciabatta, L. et al., 2016. Assessing the impact of climate-change scenarios on landslide occurrence in
686 Umbria Region, Italy. Journal of Hydrology, 541: 285-295.
687 DOI:10.1016/j.jhydrol.2016.02.007
688 Collins, B.D., Znidarcic, D., 2004. Stability analyses of rainfall induced landslides. Journal of
689 geotechnical and geoenvironmental engineering, 130(4): 362-372.
690 Croley II, T.E., Hartmann, H.C., 1985. Resolving Thiessen polygons. Journal of Hydrology, 76(3-4):
691 363-379.
692 Ewen, J., 1995. Contaminant transport component of the catchment modelling system SHETRAN.
693 Wiley, Chichester, UK.
694 Gariano, S.L. et al., 2015. Calibration and validation of rainfall thresholds for shallow landslide
695 forecasting in Sicily, southern Italy. Geomorphology, 228: 653-665.
696 DOI:10.1016/j.geomorph.2014.10.019
697 Giannecchini, R., Galanti, Y., D'Amato Avanzi, G., 2012. Critical rainfall thresholds for triggering
698 shallow landslides in the Serchio River Valley (Tuscany, Italy). Natural Hazards and Earth
699 System Science, 12(3): 829-842. DOI:10.5194/nhess-12-829-2012
700 Glade, T., Crozier, M., Smith, P., 2000. Applying probability determination to refine landslide-
701 triggering rainfall thresholds using an empirical "Antecedent Daily Rainfall Model". Pure and
702 Applied Geophysics, 157(6-8): 1059-1079.
703 Guzzetti, F., Peruccacci, S., Rossi, M., Stark, C.P., 2007. Rainfall thresholds for the initiation of
704 landslides in central and southern Europe. Meteorology and Atmospheric Physics, 98(3-4):
705 239-267. DOI:10.1007/s00703-007-0262-7
706 Guzzetti, F., Peruccacci, S., Rossi, M., Stark, C.P., 2008. The rainfall intensity–duration control of
707 shallow landslides and debris flows: an update. Landslides, 5(1): 3-17.
708 Lagomarsino, D., Segoni, S., Fanti, R., Catani, F., 2013. Updating and tuning a regional-scale landslide
709 early warning system. Landslides, 10(1): 91-97.

Lagomarsino, D. et al., 2015. Quantitative comparison between two different methodologies to define rainfall thresholds for landslide forecasting. Natural Hazards and Earth System Sciences, 15(10): 2413-2423. DOI:10.5194/nhess-15-2413-2015

Lee, S., Won, J.-S., Jeon, S.W., Park, I., Lee, M.J., 2015. Spatial landslide hazard prediction using rainfall probability and a logistic regression model. Mathematical Geosciences, 47(5): 565-589.

Lu, N., Godt, J.W., 2013. Hillslope hydrology and stability. Cambridge University Press.

Martelloni, G., Segoni, S., Fanti, R., Catani, F., 2012. Rainfall thresholds for the forecasting of landslide occurrence at regional scale. Landslides, 9(4): 485-495.

Melillo, M., Brunetti, M.T., Peruccacci, S., Gariano, S.L., Guzzetti, F., 2014. An algorithm for the objective reconstruction of rainfall events responsible for landslides. Landslides, 12(2): 311-320. DOI:10.1007/s10346-014-0471-3

Mirus, B.B., Becker, R.E., Baum, R.L., Smith, J.B., 2018. Integrating real-time subsurface hydrologic monitoring with empirical rainfall thresholds to improve landslide early warning. Landslides, 15(10): 1909-1919. DOI:10.1007/s10346-018-0995-z

Norouzi Banis, Y., Bathurst, J., Walling, D., 2004. Use of caesium-137 data to evaluate SHETRAN simulated long-term erosion patterns in arable lands. Hydrological processes, 18(10): 1795-1809.

Parkin, G., 1996. A three-dimensional variably-saturated subsurface modelling system for river basins.

Peruccacci, S. et al., 2017. Rainfall thresholds for possible landslide occurrence in Italy. Geomorphology, 290: 39-57. DOI:10.1016/j.geomorph.2017.03.031

Peruccacci, S., Brunetti, M.T., Luciani, S., Vennari, C., Guzzetti, F., 2012. Lithological and seasonal control on rainfall thresholds for the possible initiation of landslides in central Italy. Geomorphology, 139-140: 79-90. DOI:10.1016/j.geomorph.2011.10.005

Ponziani, F. et al., 2012. Assessment of rainfall thresholds and soil moisture modeling for operational hydrogeological risk prevention in the Umbria region (central Italy). Landslides, 9(2): 229-237.

735 Scheevel, C.R., Baum, R.L., Mirus, B.B., Smith, J.B., 2017. Precipitation thresholds for landslide
736 occurrence near Seattle, Mukilteo, and Everett, Washington. 2017-1039, Reston, VA.
737 DOI:10.3133/ofr20171039
738 Segoni, S., Lagomarsino, D., Fanti, R., Moretti, S., Casagli, N., 2015. Integration of rainfall thresholds
739 and susceptibility maps in the Emilia Romagna (Italy) regional-scale landslide warning system.
740 Landslides, 12(4): 773-785.
741 Segoni, S., Piciullo, L., Gariano, S.L., 2018. A review of the recent literature on rainfall thresholds for
742 landslide occurrence. Landslides. DOI:10.1007/s10346-018-0966-4
743 Segoni, S., Rossi, G., Rosi, A., Catani, F., 2014. Landslides triggered by rainfall: a semi-automated
744 procedure to define consistent intensity–duration thresholds. Computers & Geosciences, 63:
745 123-131.
746 Sidle, R.C., Ochiai, H., 2006. Landslides: processes, prediction, and land use. Water resources
747 monograph series.
748 Staley, D.M., Kean, J.W., Cannon, S.H., Schmidt, K.M., Laber, J.L., 2013. Objective definition of
749 rainfall intensity–duration thresholds for the initiation of post-fire debris flows in southern
750 California. Landslides, 10(5): 547-562.
751 Zhang, J., Han, D., 2017. Catchment Morphing (CM): A novel approach for runoff modeling in
752 ungauged catchments. Water Resources Research, 53(12): 10899-10907.
753 Zhang, R., Santos, C.A., Moreira, M., Freire, P.K., Corte-Real, J., 2013. Automatic calibration of the
754 SHETRAN hydrological modelling system using MSCE. Water resources management, 27(11):
755 4053-4068.

756